Electronic Supplementary Material (ESI) for CrystEngComm.
This journal is © The Royal Society of Chemistry 2018

Supporting Information

Halogen Bonds in 2,5-Dihalopyridine-Copper(II) Chloride Complexes

Rakesh Puttreddy,[a] Carolina von Essen,[a] Anssi Peuronen,[a] Manu Lahtinen[a] and Kari Rissanen[a]

[a] *University of Jyvaskyla, Department of Chemistry, P. O. Box 35, FI-40014 Jyvaskyla, Finland*

Table of Contents

I General Information

All the solvents used for crystal growth are reagent grade and are used as received. The ligands, 2-chloro-5-fluoropyridine (**1**) 2,5-dichloropyridine (**2**), 5-bromo-2-chloropyridine (**3**), 2-chloro-5-iodopyridine (**4**), 2-bromo-5-fluoropyridine (**5**), 2-bromo-5-chloropyridine (**6**), 2,5-dibromopyridine (**7**) , 2-bromo-5-iodopyridine (**8**) and 3-iodopyridine (3IPy) were purchased from TCI Chemicals Europe. Infrared spectra were recorded using Bruker instrument by pressing a small amount of the sample on the diamond ATR Prism. Melting points were recorded using Stuart Scientific SMP3II melting point apparatus.

II Synthesis of 2,5-dihalopyridine-Cu(II) complexes

IIa General synthesis of 2,5-dihalopyridine-Cu(II) complexes

To a solution of $CuCl_2.2H_2O$ (0.088 mmol) in acetonitrile (1.0 ml), was added respective 2,5-dihalopyridine (0.176 mmol) dissolved in acetonitrile (0.5 ml) at room temperature. In case of precipitation, the samples were briefly (1-2 minutes) heated over 40°C hot plate to clear solutions. The solutions were left at room temperature, and subjected to slow evaporation to give single crystals suitable for X-ray analysis.

IIb. (**1**)$_4$·[$CuCl_2$]$_2$: IR ν_{max} cm^{-1}: 3085, 3020, 2921, 2849, 1597, 1570, 1460, 1369, 1243, 1112, 1034, 852, 836, 720, 632, 525, 442. mp: > 303 °C

IIc. (**2**)$_4$·[$CuCl_2$]$_2$: IR ν_{max} cm^{-1}: 3085, 3052, 2921, 2918, 2849, 1578, 1449, 1431, 1353, 1273, 1128, 1031, 929, 846, 828, 720, 651, 560, 506, 447. mp: > 303 °C

IId. (**3**)$_4$·[$CuCl_2$]$_2$: IR ν_{max} cm^{-1}: 3087, 2929, 2851, 1570, 1449, 1345, 1034, 1144, 1117, 919, 833, 712, 651, 522, 436, 434. mp: > 303 °C

IIe. Bulk sample of (**4.1**)$_4$·[$CuCl_2$]$_2$ and (**4.2**)$_2$·$CuCl_2$: IR ν_{max} cm^{-1}: 3093, 1562, 1450, 1342, 1144, 1106, 1031, 921, 839, 720, 648, 498, 431. mp: > 303 °C

IIf. Bulk sample of Complex (**5.1**)$_4$·[$CuCl_2$]$_2$ and (**5.2**)$_2$·$CuCl_2$: IR ν_{max} cm^{-1}: 3361, 3079, 3015, 2621, 2854, 1583, 1374, 1455, 1251, 1208, 1098, 1031, 919, 844, 715, 597, 530, 447, 428. mp: > 303 °C

IIg. Complex (**6**)$_2$·$CuCl_2$: IR ν_{max} cm^{-1}: 3058, 3055, 1573, 1455, 1353, 1273, 1235, 1136, 1120, 1045, 911, 833, 771, 707, 645, 501, 436. mp: > 303 °C

IIh. Complex (**7**)$_2$·$CuCl_2$:IR ν_{max} cm^{-1}: 3093, 2913, 2846, 1567, 1439, 1273, 1356, 1104, 1037, 911, 825, 747, 704, 648, 495, 428. mp: > 303 °C

IIi. Complex (**8**)$_2$·$CuCl_2$: IR ν_{max} cm^{-1}: 3093, 2921, 2849, 1559, 1439, 1356, 1275, 1104, 1034, 913, 817, 710, 648, 482, 431. mp: > 303 °C

IIj. Complex (3IPy)$_2$·$CuCl_2$: IR ν_{max} cm^{-1}: 3356, 1583, 1559, 1454, 1316, 1185, 1077, 1045, 1007, 795, 695, 614, 438. mp: > 303 °C

III Solid-state X-ray crystallography

IIIa. X-ray Crystal structure analyses

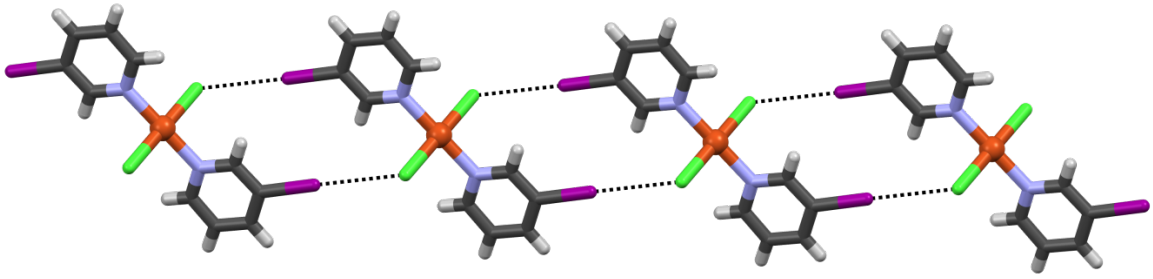

Figure S1. Section of crystal packing in $(3IPy)_2{\cdot}CuCl_2$ to display of 1-D polymer structure extended *via* C5–I5···Cl–Cu halogen bonds.

IIIb. X-ray experimental details

The crystal data and experimental details for the data collections are given in Table S1 - S3. Single-crystal X-ray data for $(\mathbf{1})_4{\cdot}[CuCl_2]_2$, $(\mathbf{2})_4{\cdot}[CuCl_2]_2$, $(\mathbf{3})_4{\cdot}[CuCl_2]_2$, $(\mathbf{4.1})_4{\cdot}[CuCl_2]_2$, $(\mathbf{4.2})_2{\cdot}CuCl_2$, $(\mathbf{5.1})_4{\cdot}[CuCl_2]_2$, $(\mathbf{5.2})_2{\cdot}CuCl_2$, $(\mathbf{6})_2{\cdot}CuCl_2$ and $(\mathbf{8})_2{\cdot}CuCl_2$ were measured on a Bruker-Nonius Kappa CCD diffractometer with an APEX-II CCD detector using graphite-monochromated Mo-Kα (*λ* = 0.71073 Å) radiation. The data for $(\mathbf{7})_2{\cdot}CuCl_2$ was measured using a Rigaku SuperNova dual-source Oxford diffractometer equipped with an Atlas detector using mirror-monochromated Cu-*K*α (λ = 1.54184 Å) radiation. The data for $(3IPy)_2{\cdot}CuCl_2$ was collected using a Rigaku SuperNova single-source Oxford diffractometer with an Atlas EoS CCD detector using mirror-monochromated Mo-Kα (λ = 0.71073 Å) radiation. The data collection and reduction for data sets collected using Rigaku instruments were performed using the program *CrysAlisPro*[1] and Gaussian face index absorption correction method[1] was applied. For the data obtained using Bruker Nonius Kappa diffractometer processing was performed using the program COLLECT[2] and HKL DENZO AND SCALEPACK.[3] The intensities for data collected by Bruker Nonius Kappa diffractometer were corrected for absorption using SADABS[4] with multi-scan absorption correction type method. All structures were solved with direct methods (*SHELXS*)[5] and refined by full-matrix least squares on F^2 using the *OLEX2* software[6], which utilizes the *SHELXL*-2013 module.[5]

Table S1. Single crystal X-ray experimental details for (**1**)$_4$·[$CuCl_2$]$_2$, (**2**)$_4$·[$CuCl_2$]$_2$, (**3**)$_4$·[$CuCl_2$]$_2$ and (**4.1**)$_4$·[$CuCl_2$]$_2$

Complex	(**1**)$_4$·[$CuCl_2$]$_2$	(**2**)$_4$·[$CuCl_2$]$_2$	(**3**)$_4$·[$CuCl_2$]$_2$	(**4.1**)$_4$·[$CuCl_2$]$_2$
CCDC No:	1821327	1821328	1821329	1821330
Empirical formula	$C_{20}H_{12}Cl_8Cu_2F_4N_4$	$C_{20}H_{12}Cl_{12}Cu_2N_4$	$C_{20}H_{12}Br_4Cl_8Cu_2N_4$	$C_{20}H_{12}Cl_8Cu_2I_4N_4$
Formula weight	519.33	860.82	1038.66	1226.62
Temperature (K)	170.0(1)	170.0(1)	170.0(1)	170.0(1)
Crystal system	Triclinic	Monoclinic	Monoclinic	Monoclinic
Space group	*P*-1	*I*2/*a*	*I*2/*m*	*I*2/*m*
Unit cell dimensions: a (Å)	7.4310(15)	14.396(3)	7.8894(16)	8.0829(16)
Unit cell dimensions: b (Å)	8.7786(18)	14.183(3)	14.316(3)	14.605(3)
Unit cell dimensions: c (Å)	10.589(2)	15.458(3)	13.494(3)	13.664(3)
Unit cell dimensions: α (°)	87.15(3)	90	90	90
Unit cell dimensions: β (°)	82.23(3)	114.23(3)	92.06(3)	91.89(3)
Unit cell dimensions: γ (°)	82.29(3)	90	90	90
Volume / Å^3	677.9(2)	2878.2(12)	1523.1(5)	1612.1(6)
Z	1	4	2	2
Density (calculated) mg/m^3	1.947	1.987	2.265	2.527
Absorption Coefficient mm^{-1}	2.405	2.614	7.367	5.833
F(000)	390	1688	988	267
Crystal size (mm^3)	0.17x0.11x 0.11	0.22x0.19x 0.19	0.24x0.19x 0.14	0.27x0.23 x 0.23
θ range for data collection (°)	2.34 to 25.24	2.12 to 25.24	2.85 to 25.24	2.05 to 25.24
Reflections collected	4433	7740	4917	7375
[R(int)]	[0.0299]	[0.0219]	[0.0279]	[0.0263]
Reflections [I>2sigma(I)]	1968	2338	1299	1423
Data completeness (%)	99.50	99.20	99.99	95.99
Data/ restraints/ parameters	2443/0/172	2582/0/172	1448/0/91	1516/0/91
Goodness-of-fit on F^2	1.063	1.037	1.051	1.067
Final R_1 indices [I>2sigma(I)]	R_1 = 0.0406 wR_2 = 0.0825	R_1 = 0.0202 wR_2 = 0.0503	R_1 = 0.0212 wR_2 = 0.0450	R_1 = 0.0192 wR_2 = 0.0430
Final R indices [all data]	R_1 = 0.0559 wR_2 = 0.0887	R_1 = 0.0237 wR_2 = 0.0520	R_1 = 0.0259 wR_2 = 0.0466	R_1 = 0.0215 wR_2 = 0.0440
Largest diff. peak/hole (e.Å^{-3})	0.438/ -0.561	0.364/ -0.284	0.362/ -0.376	0.561/ -0.678

Table S2. Single crystal X-ray experimental details for (**4.2**)$_2$·$CuCl_2$, (**5.1**)$_4$·$[CuCl_2]_2$, (**5.2**)$_2$·$CuCl_2$ and (**6**)$_2$·$CuCl_2$

Complex	(**4.2**)$_2$·$CuCl_2$	(**5.1**)$_4$·$[CuCl_2]_2$	(**5.2**)$_2$·$CuCl_2$	(**6**)$_2$·$CuCl_2$
CCDC No:	1821331	1821332	1821333	1821334
Empirical formula	$C_{10}H_6Cl_4CuI_2N_2$	$C_{20}H_{12}Br_4Cl4Cu_2F_4N_4$	$C_{10}H_6Br_2Cl_2CuF_2N_2$	$C_{10}H_6Br_2Cl_4CuN_2$
Formula weight	613.31	972.86	486.43	519.33
Temperature (K)	170.0(1)	170.0(1)	170.0(1)	170.0(1)
Crystal system	Monoclinic	Monoclinic	Monoclinic	Monoclinic
Space group	*C*2/*c*	*C*2/*m*	*P*2$_1$/*c*	*C*2/*c*
Unit cell dimensions: a (Å)	8.3678(17)	14.946(3)	5.7104(11)	8.1656(16)
Unit cell dimensions: b (Å)	13.106(3)	15.233(3)	11.981(2)	12.708(3)
Unit cell dimensions: c (Å)	14.700(3)	6.7384(13)	10.478(2)	14.591(3)
Unit cell dimensions: α (°)	90	90	90	90
Unit cell dimensions: β (°)	90.12(3)	91.82(3)	103.66(3)	91.79(3)
Unit cell dimensions: γ (°)	90	90	90	90
Volume / Å^3	1612.1(6)	1533.4(5)	696.6(3)	1513.4(5)
Z	4	2	2	4
Density (calculated) mg/m^3	2.527	2.107	2.319	2.279
Absorption Coefficient mm^{-1}	5.834	6.990	7.694	7.414
F(000)	1132	924	462	988
Crystal size (mm^3)	0.14x0.09x 0.09	0.13x0.13x 0.10	0.13x0.12x 0.09	0.20x0.16x 0.13
θ range for data collection (°)	2.77 to 25.24	2.67 to 25.25	2.63 to 25.22	3.0 to 25.24
Reflections collected	9133	4678	5238	2880
[R(int)]	[0.0412]	[0.0270]	[0.0366]	[0.0208]
Reflections [I>2sigma(I)]	1629	1320	1112	1224
Data completeness (%)	99.90	99.40	98.80	97.90
Data/ restraints/ parameters	2009/0/87	1436/0/91	1260/0/88	1341/0/87
Goodness-of-fit on F^2	1.020	1.079	1.042	1.060
Final R_1 indices [I>2sigma(I)]	R_1 = 0.0291 wR_2 = 0.0503	R_1 = 0.0197 wR_2 = 0.0473	R_1 = 0.0206 wR_2 = 0.0471	R_1 = 0.0237 wR_2 = 0.0526
Final R indices [all data]	R_1 = 0.0434 wR_2 = 0.0537	R_1 = 0.0226 wR_2 = 0.0483	R_1 = 0.0261 wR_2 = 0.0488	R_1 = 0.0277 wR_2 = 0.0543
Largest diff. peak/hole (e.Å^{-3})	0.455/ -0.495	0.275/ -0.372	0.299/ -0.322	0.332/ -0.371

Table S3. Single crystal X-ray experimental details for (**7**)$_2$·$CuCl_2$, (**8**)$_2$·$CuCl_2$ and (3IPy)$_2$·$CuCl_2$

Complex	(**7**)$_2$·$CuCl_2$	(**8**)$_2$·$CuCl_2$	(3IPy)$_2$·$CuCl_2$
CCDC No:	1821335	1821336	1821338
Empirical formula	$C_{10}H_6Br_4Cl_2CuN_2$	$C_{10}H_6Br_2Cl_2CuI_2N_2$	$C_{10}H_8Cl_2CuI_2N_2$
Formula weight	608.25	702.23	544.42
Temperature (K)	120.00(10)	170.0(1)	120.0(1)
Crystal system	Monoclinic	Monoclinic	Triclinic
Space group	*C*2/*c*	*C*2/*c*	*P*-1
Unit cell dimensions: a (Å)	8.2021(4)	8.4827(17)	4.0102(7)
Unit cell dimensions: b (Å)	12.8425(7)	13.075(3)	8.4892(13)
Unit cell dimensions: c (Å)	14.6338(6)	14.721(3)	10.1403(13)
Unit cell dimensions: α (°)	90	90	90.863(12)
Unit cell dimensions: β (°)	91.109(5)	90.35(3)	92.738(13)
Unit cell dimensions: γ (°)	90	90	97.811(14)
Volume / Å^3	1541.17(13)	1632.7(6)	341.54(9)
Z	4	4	1
Density (calculated) mg/m^3	2.621	2.857	2.647
Absorption Coefficient mm^{-1}	17.233	10.328	6.487
F(000)	1132	1276	251
Crystal size (mm^3)	0.10x0.07x 0.04	0.17x0.11x 0.11	0.12x0.03x 0.03
θ range for data collection (°)	6.05 to 66.75	2.77 to 25.24	3.12 to 25.24
Reflections collected [R(int)]	6858 [0.0602]	8216 [0.0350]	2007 [0.0246]
Reflections [I>2sigma(I)]	1258	1755	1126
Data completeness (%)	98.90	99.99	99.57
Data/ restraints/ parameters	1364/0/87	2027/0/87	1231/0/79
Goodness-of-fit on F^2	1.077	1.051	1.092
Final R_1 indices [I>2sigma(I)]	R_1 = 0.0419 wR_2 = 0.1009	R_1 = 0.0243 wR_2 = 0.0495	R_1 = 0.0263 wR_2 = 0.0582
Final R indices [all data]	R_1 = 0.0446 wR_2 = 0.1032	R_1 = 0.0316 wR_2 = 0.0514	R_1 = 0.0307 wR_2 = 0.0608
Largest diff. peak/hole (e.Å^{-3})	0.888/ -0.780	0.593/ -0.658	1.162/ -0.607

IV X-ray Powder diffraction analysis

The bulk samples of complexes (**1**)$_4$·[$CuCl_2$]$_2$ - (**8**)$_4$·[$CuCl_2$]$_2$ were analysed by powder X-ray diffraction (PXRD) technique using a PANalytical X'Pert PRO Alpha 1 diffractometer with Cu $K_{\alpha 1}$ radiation (1.54060 Å; 45 kV, 40 mA). The samples were measured using a silicon-made zero-background signal sample holder, onto which the each sample was prepared using petrolatum jelly as an adhesive. Diffraction intensities were recorded by an X'Celerator detector at room temperature with 2θ-range of 3–70° with a step size of 0.017° and counting times of 120 s per step. Raw data was handled with X´pert HighScore Plus v. 4.6 program. The unit cell parameters of the samples were determined by Pawley analysis[7] within DASH program package[8] using the corresponding single crystal structure parameters as the basis of least-squares refinements (variable parameters were as follows: zero-offset, unit cell and peak profile parameters). The fitted diffraction graphs, refined unit cells and resulting R-factors/goodness-of-fits are shown in figures **S3**-**S10** and in table **S4**, respectively.

Pawley analysis shows that the refined lattice parameters of the bulk powders have good agreement with their corresponding single crystal structures (PXRD derived unit cells are ca. 2 % larger in volume compared to SCXRD data due to the thermal expansion effects caused by the difference in data collection temperature between PXRD and SCXRD). In the case of complexes of ligands **4** and **5**, with which both monomeric and dimeric single crystal structures were obtained, the PXRD analysis clearly shows that for **4** the bulk material corresponds to the dimeric complex, (**4.1**)$_4$·[$CuCl_2$]$_2$, whereas ligand **5** gives the monomeric complex, (**5.2**)$_4$·[$CuCl_2$]$_2$, as the bulk product. In samples of (**3**)$_4$·[$CuCl_2$]$_2$ and (**6**)$_4$·$CuCl_2$, a small amount of impurity is observed as weak peaks emerging from the baseline which do not correspond to the simulated pattern or to the powder patterns of the starting materials. Hence, they are most likely a result of minor amounts of monomer/dimer complexes, *i.e.* (**3**)$_4$·$CuCl_2$ and (**6**)$_4$·[$CuCl_2$]$_2$, formed in the synthesis of major products, (**3**)$_4$·[$CuCl_2$]$_2$ and (**6**)$_4$·$CuCl_2$, respectively.

Table S4. Results of the powder X-ray diffraction Pawley analysis of complexes (**1**)·$[CuCl_2]_2$ - (**8**)·$CuCl_2$ and comparison between the refined unit cell parameters of bulk powders (PXRD, at 293 K) and single crystal structures (SCXRD, at 120-170 K).

	1-SCXRD	**1-PXRD**	**2-SCXRD**	**2-PXRD**	**3-SCXRD**	**3-PXRD**	**4.1-SCXRD**	**4.1-PXRD**
a /Å	7.4310(15)	7.50901(23)	16.234(3)	16.43543(96)	15.384(3)	15.53019(37)	8.0829(16)	8.11049(14)
b /Å	8.7786(18)	8.83062(17)	14.183(3)	4.18905(24)	14.316(3)	14.31825(12)	14.605(3)	14.60767(21)
c /Å	10.589(2)	10.69961(20)	14.396(3)	14.5687(13)	7.8894(16)	7.94399(90)	13.664(3)	13.75549(24)
α /°	87.15(3)	87.3908(12)	90	90	90	90	90	90
β /°	82.23(3)	80.994(1)	119.74(3)	120.1735(32)	118.77(3)	118.3963(18)	91.89(3)	92.0617(10)
γ /°	82.29(3)	82.3337(13)	90	90	90	90	90	90
V /Å^3	678	694	2878	2937	1523	1554	1612	1629
χ^2	-	4.8895	-	4.4336	-	12.5020	-	3.6056
$R_{expected}$	-	8.32	-	4.90	-	5.77	-	7.78
$R_{profile}$	-	18.40	-	10.33	-	20.39	-	14.77
	5.2-SCXRD	**5-PXRD**	**6-SCXRD**	**6-PXRD**	**7-SCXRD**	**7-PXRD**	**8-SCXRD**	**8-PXRD**
a /Å	5.7104(11)	5.69285(46)	8.1656(16)	8.22702(14)	8.2021(4)	8.31654(23)	8.4800(17)	8.57737(28)
b /Å	11.981(2)	12.01278(18)	12.708(3)	12.73200(17)	12.8425(7)	12.87389(35)	13.068(3)	13.11588(45)
c /Å	10.478(2)	10.68773(29)	14.591(3)	14.60465(27)	14.6338(6)	14.63652(45)	14.716(3)	14.73350(52)
α /°	90	90	90	90	90	90	90	90
β /°	103.66(3)	103.4794(17)	91.79(3)	91.6370(11)	91.109(5)	90.8610(15)	90.38(3)	90.5778(16)
γ /°	90	90	90	90	90	90	90	90
V /Å^3	697	711	1513	1529	1541	1567	1631	1657
χ^2	-	4.4019	-	4.6596	-	3.7945	-	2.0461
$R_{expected}$	-	9.99	-	6.54	-	6.33	-	8.72
$R_{profile}$	-	20.96	-	14.11	-	12.33	-	12.47

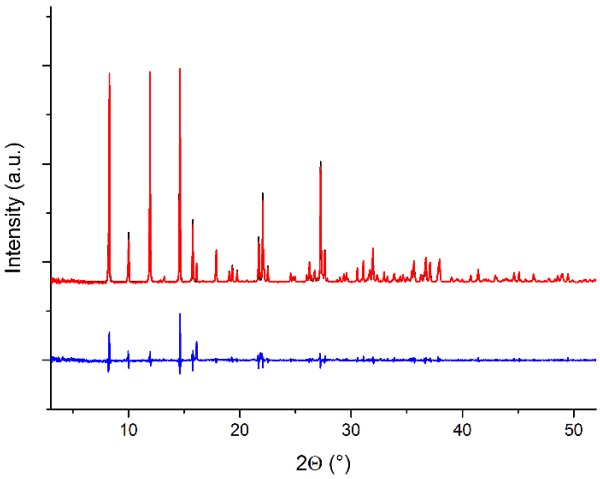

Figure S2. Pawley refinement graphs for the bulk material, obtained in the reaction between **1** and $CuCl_2$, with refined profile in red, measured PXRD data in black and the difference plot in blue.

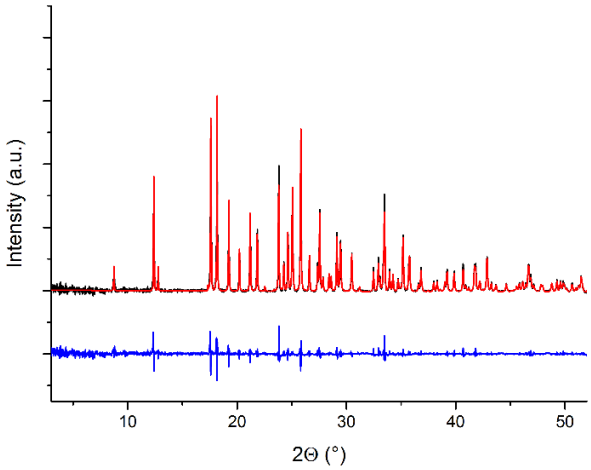

Figure S5. Pawley refinement graphs for the bulk material, obtained in the reaction between **4** and $CuCl_2$, with refined profile in red, measured PXRD data in black and the difference plot in blue.

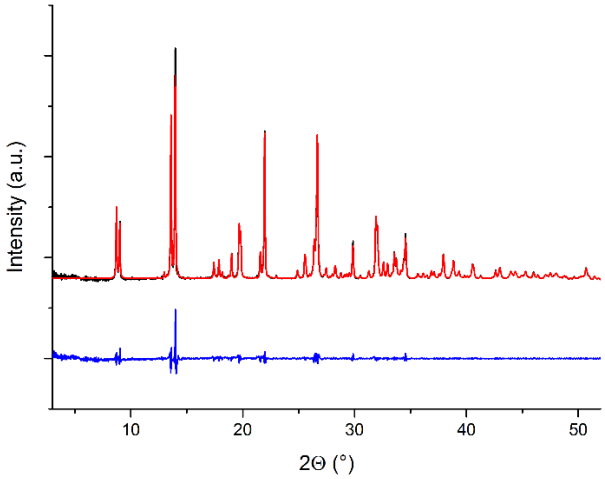

Figure S3. Pawley refinement graphs for the bulk material, obtained in the reaction between **2** and $CuCl_2$, with refined profile in red, measured PXRD data in black and the difference plot in blue.

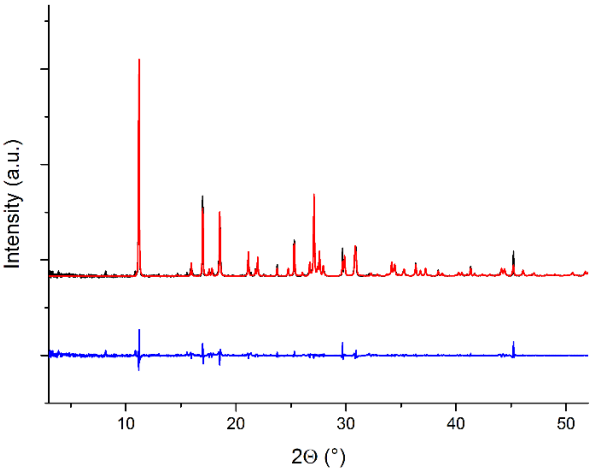

Figure S6. Pawley refinement graphs for the bulk material, obtained in the reaction between **5** and $CuCl_2$, with refined profile in red, measured PXRD data in black and the difference plot in blue.

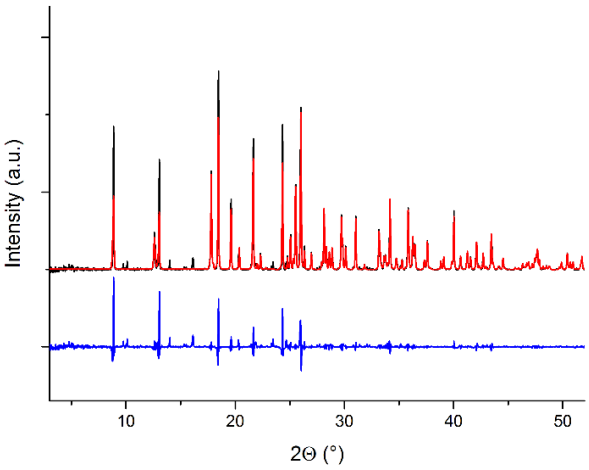

Figure S4. Pawley refinement graphs for the bulk material, obtained in the reaction between **3** and $CuCl_2$, with refined profile in red, measured PXRD data in black and the difference plot in blue.

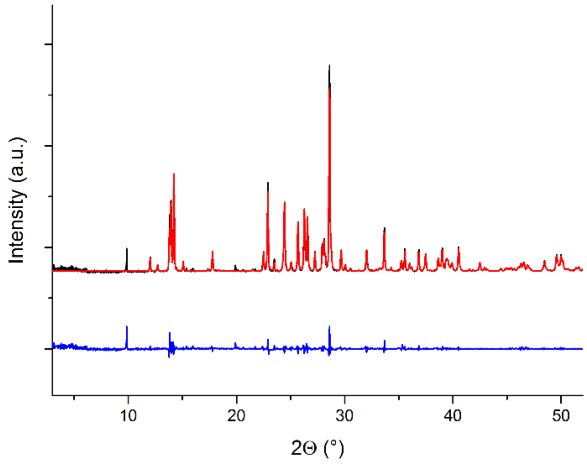

Figure S7. Pawley refinement graphs for the bulk material, obtained in the reaction between **6** and $CuCl_2$, with refined profile in red, measured PXRD data in black and the difference plot in blue.

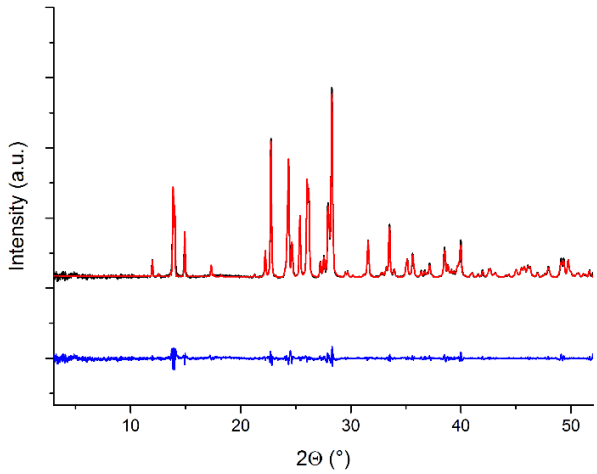

Figure S8. Pawley refinement graphs for the bulk material, obtained in the reaction between **7** and $CuCl_2$, with refined profile in red, measured PXRD data in black and the difference plot in blue.

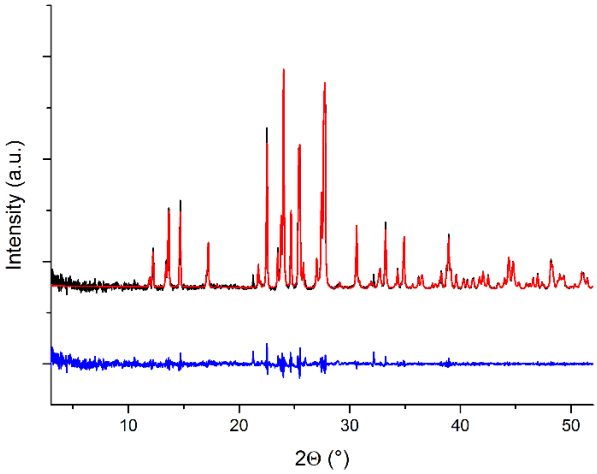

Figure S9. Pawley refinement graphs for the bulk material, obtained in the reaction between **8** and $CuCl_2$, with refined profile in red, measured PXRD data in black and the difference plot in blue.

V References

(1) *Rigaku Oxford Diffraction 2015*, *CrysAlisPro* Version 1.171.38.43.
(2) Bruker AXS BV, Madison, WI, USA; 1997–2004.
(3) Z. Otwinowski, W. Minor, *Methods Enzymol.,* 1997, **276**, 307–326.
(4) R. H. Blessing, *J. Appl. Cryst.,* 1997, **30**, 421–426.
(5) (a) G. M. Sheldrick, G. M. *Acta Cryst.,* 2008, **A64**, 112–122; (b) Sheldrick, G.M., *Acta Cryst.*, 2015, **A71**, 3-8; (c) Sheldrick, G.M., *Acta Cryst.*, 2015, **C71**, 3-8.
(6) O. V. Dolomanov, L. J. Bourhis, R. J. Gildea, J. A. K. Howard, H. J. Puschmann, *J. Appl. Cryst.,* 2009, **42**, 339–341.
(7) G.S. Pawley, *J. Appl. Cryst.*, 1981, **14**, 357–361.
(8) W. I. F. David, K. Shankland, J. van de Streek, E. Pidcock, W. D. S. Motherwell, J. C. Cole, *J. Appl. Cryst.*, 2006, **39**, 920–915.